Multiple-Beam Fiber-Optic Beamformer With Binary Array of Delay Lines

S. Granieri, M. Jaeger, and A. Siahmakoun, *Member, IEEE*

***Abstract*—A multibeam optical beamformer capable of controlling a phased-array antenna in receive/transmit mode is proposed. The processor can be programmed to sweep the antenna aperture following an independent angular sequence for each radio-frequency (RF) beam. A two-beam two-channel 3-bit version of the beamformer has been experimentally demonstrated. The optical beamformer processes two independent RF beams, for eight different angular directions, and it is based on a binary array of three delay lines. Each delay line is composed of four fiber Bragg gratings whose center wavelengths are channels 30 to 33 of the International Telecommunications Union (ITU) grid. Measurements are performed for both receive and transmit modes and for RF values between 0.5 and 1.5 GHz. We present beam-pattern results showing the squint-free performance of the beamformer within this frequency range. In the transmit mode, two RF beams are steered and characterized for a broadside target position. In the receive mode, the beamformer performance is characterized by detecting two simultaneous RF beams.**

***Index Terms*—Fiber Bragg gratings, optical beamforming, radio-frequency (RF) photonics, true-time delay.**

I. Introduction

PRESENT phased-array antennas are controlled by digital microwave phase-shifting devices with limited bandwidth. For large arrays, electronic radar architectures become hardware intensive, resulting in bulky and heavy systems. However, modern radar applications demand large instantaneous bandwidth with frequency independent beam steering. The solution involves digitally controlled true-time delay (TTD) antenna arrays. In conventional radio-frequency (RF) systems, TTD is achieved by switching to a different lengths of electrical cable. However, these systems tend to be bulky, heavy, and susceptible to electromagnetic interference. The use of photonics for phased-array antennas control is an active field of research, which has helped to overcome some of the problems mentioned above. Photonic systems can provide a lightweight, compact, low-cost phased-array antenna processor, which is immune to electromagnetic interference. Several optical approaches for both phase-based and true-time delay type antenna control have been proposed [1]. Although the optoelectronic phase-based systems are directed toward replacing present narrow-band phased arrays, the TTD systems are geared toward the wide instantaneous bandwidth radars requiring wide-band signal processing capabilities in L and C bands.

Manuscript received April 17, 2003; revised June 26, 2003. This work was supported by the Office of Naval Research under Contract N00014-00-0782.

The authors are with the Department of Physics and Optical Engineering, Rose-Hulman Institute of Technology, Terre Haute, IN 47803 USA.

Digital Object Identifier 10.1109/JLT.2003.821733

Fiber optics has been used in applications for providing optical time delays. A possible approach to achieve different time delays is to use a binary delay line configuration in which the optical signal is routed by optical switches through the lines to obtain selected delays [2]. The use of ternary architectures in optical beamformers and programmable arrays of delay lines is considered in [3], [4]. To introduce time delays between RF signals, optical beamforming networks can also take advantage of wavelength-division multiplexing (WDM) encoding. RF signals from/to each transmit/receive (T/R) element of the antenna are coded using optical carriers with different wavelengths. Thus, different time delays can be introduced between different optical carriers using wavelength-dependent components such as fiber Bragg gratings (FBG) or high-dispersion fiber [5]–[9]. Using the last technique, a beamformer capable of processing independent RF beams in receive mode is demonstrated [10].

A spatial optical processor for controlling a phased-array antenna has been studied in [11]. Two-dimensional Fourier transforms can be performed optically in real time by far-field diffraction of coherent light. Non-TTD beamforming is possible by illuminating a mask that represents a scaled down replica of the desired antenna beam. Thus, the spatial optical beamformer controls the phase of the antenna elements. This approach is used to design optical processors to drive a multibeam antenna array in transmit mode [12] as well as in receive mode [13], [14]. All these systems require coherent configurations in the detection stage. An optical beamformer for multiple simultaneous beams in transmit mode using bulk optics and acoustooptic modulation is proposed and demonstrated in [15].

The present paper describes a novel optical beamformer that allows TTD control of multiple simultaneous RF beams exploiting WDM technology. The RF signals, which feed the T/R elements of the phased antenna array, are coded using optical carriers with different wavelengths. The beamformer is based on a binary array of optical delay lines. Delay lines which are constructed by a sequence of FBG, are interconnected by standard fiber components such as optical switches and circulators. Multiple beam processing is achieved by encoding signals associated with each RF beam by a different WDM optical channel. This allows the beamformer to receive and transmit each beam independently with a wide variety of programmable time delays. The flexibility of this approach is noticed by the fact that each RF beam can be swept independently following its own angular sequence in the antenna. The proposal is demonstrated for a binary version of a two-channel 3-bit programmable dispersion matrix (PDM) that controls a two-beam optical beamformer in the T/R mode.

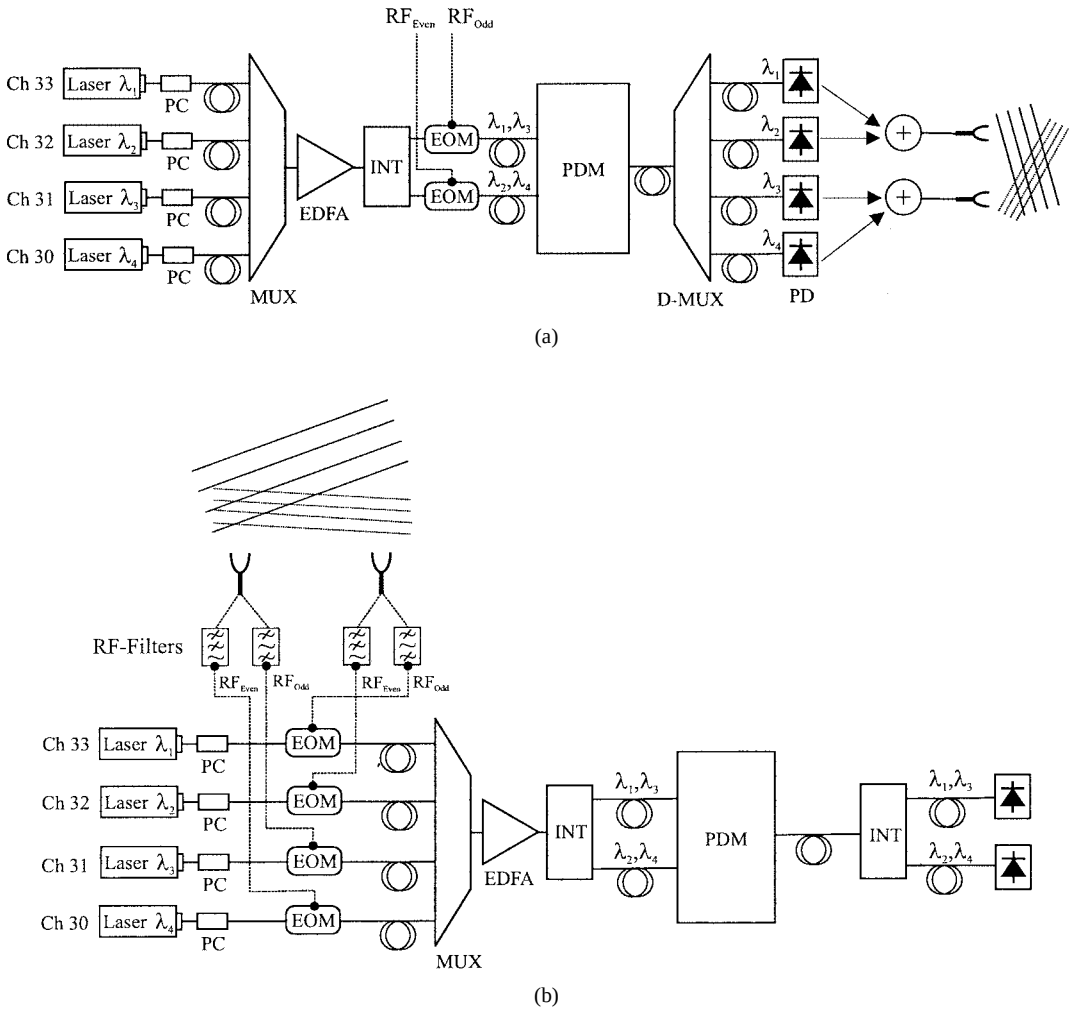

Fig. 1. Two-beam two-channel optical beamformer. (a) Transmit mode configuration. (b) Receive mode configuration. The resolution of the proposed system is 3-bit. PC: Polarization controller, EOM: electrooptic modulator, PD: Photodetector, INT: interleaver.

In Section II, we describe a two-beam two-channel optical beamformer and the generalization for an M-beams N-channels prototype. System characterization showing the squint-free performance and design parameters are discussed in Section III. In Sections IV and V, we present beam-pattern measurement results for two simultaneous RF beams in transmit and receive modes, respectively. Finally, concluding remarks are given in Section VI.

II. System Description

Fig. 1 shows a schematic drawing of the two-beam beamformer architecture that is able to drive a two-element array antenna. Four diode lasers provide optical carriers/channels with wavelengths λ_1 to λ_4. In the present approach, each pair of even (λ_2 and λ_4) and odd (λ_1 and λ_3) optical channels carries information of one RF beam independently. The RF beam, which is controlled by the odd (even) optical channels, is referred as the odd (even) RF beam.

In the transmission regime, the combined even and odd channels are then separately modulated with RF signals using two electrooptic modulators (EOMs) as shown in Fig. 1(a). Modulation of multiplexed channels ensures zero phase delay between the RF signals before the optical carriers are processed. The RF signals modulated on the even and odd channels are in phase. The modulated optical carriers feed the PDM, which performs the true-time delay processing. The PDM is capable of providing independent time delays for the even and odd channels. For each configuration of the PDM, λ_2 lags λ_4 and λ_1 lags λ_3 by an independent time period. At the output of the PDM, after the proper phase difference is set, optical signals are demultiplexed. Four broad-band photodetectors, in a direct detection configuration, recover the processed RF signals. Then the RF signals are linearly combined and amplified before feeding the antenna T/R elements.

The schematic of the two-beam optical beamformer in receive mode is shown in Fig. 1(b). Incoming RF beams from two targets with different frequencies are received by two antenna-array elements. RF bandpass filters split the signal at each antenna element according to their frequency. Even and odd optical channels are modulated by the signals RF_{Even} and RF_{Odd}, respectively. The phase difference of each RF beam at the antenna elements depends on the target angular position. The time delay between the even and odd multiplexed optical channels is corrected independently by the PDM and detected with a single photodetector. The output power of each photodetector is a func-

tion of the corrected phase difference between the RF signals for each beam

$$P_{\mathrm{Even}}(\mathrm{dB}) = 10\log\left(K_{\mathrm{I}} + K_{\mathrm{II}}\cos\Delta\varphi_{\mathrm{Even}}\right) \quad (1a)$$

$$P_{\mathrm{Odd}}(\mathrm{dB}) = 10\log\left(K_{\mathrm{III}} + K_{\mathrm{IV}}\cos\Delta\varphi_{\mathrm{Odd}}\right) \quad (1b)$$

where $\Delta\varphi_{\mathrm{Even}}$ and $\Delta\varphi_{\mathrm{Odd}}$ are the phase differences of each RF signal after the PDM and K_{I}, K_{II}, K_{III}, K_{IV} are the proportionality constants which depend on the power of the optical carriers. Thus, the output power in each photodetector is related to each target angular position via this phase difference. When the PDM properly corrects for the phase difference at the antenna elements, a maximum power will be detected for a given target position.

A two-beam two-channel version of the PDM is shown in Fig. 2(a). The PDM consist of three delay lines capable of controlling an antenna array of two T/R elements. It can produce eight different delay configurations for each beam (3-bit resolution), thus, it is capable of pointing the even an odd RF beams independently in eight different angular directions. In general, the 2^N delay configuration (N-bit) version consists of an array of N delay lines. Each delay line consists of four FBG, where the center wavelength of each FBG matches one of the multiplexed optical channels. The separation between FBG with center wavelengths corresponding to either channels (odd or even), is increased in multiples of two from delay line to delay line. Thus, time delays between channels are proportional to these FBG separations. The separation of two adjacent gratings corresponding to the even and odd channels of the ith line are given by

$$\Delta L_{i,\mathrm{Even}} = 2^{i-1}\Delta L_{1,\mathrm{Even}} \quad (2a)$$

$$\Delta L_{i,\mathrm{Odd}} = 2^{i-1}\Delta L_{1,\mathrm{Odd}} \quad (2b)$$

where $\Delta L_{1,\mathrm{Even}}$ and $\Delta L_{1,\mathrm{Odd}}$ are the minimum separations between the Bragg gratings which correspond to the even and odd channels of line 1, respectively. Using (2), the time delay provided by the ith line for the odd and even channels can be written as

$$\tau_{i,\mathrm{Even}} = \frac{2n_{\mathrm{eff}}\Delta L_{i,\mathrm{Even}}}{c} \quad (3a)$$

$$\tau_{i,\mathrm{Odd}} = \frac{2n_{\mathrm{eff}}\Delta L_{i,\mathrm{Odd}}}{c} \quad (3b)$$

where n_{eff} is the effective refraction index of the fiber and c is the speed of light. The programmable switch units route the even and odd channels independently from each other through the PDM. Each switch unit consists of two 1×2 switches and two 1×2 couplers. The upper switch in the subset shown in Fig. 2(a) directs the odd channels either to the delay line, for introducing a time delay between the channels, or to bypass the delay line. While the lower switch in Fig. 2(a) performs similar function for the even channels. The 1×2 couplers are used to combine the outputs from both switches; those either going to the delay or bypass lines. Such couplers have an insertion loss of 3 dB. Circulators route the optical channels to/from the delay lines. A 1×2 coupler is used to combine the optical signals coming from the delay line and the bypass line for a second time. After the 1×2 coupler, an interleaver is used to separate the four multiplexed channels again into odd and even channels. The interleaver is followed by a switch unit that is connected to the next delay line. This structure repeats itself until the 1×2 coupler after the last delay line. With this configuration, only positive time delays are possible. This means λ_2 always lags λ_4 and λ_1 always lags λ_3 by a time period. The two RF beams, which are generated by these time delays, can only be steered in positive angular directions. The achievable steering angles $\phi_{m,\mathrm{Even}}$ and $\phi_{m,\mathrm{Odd}}$ for the even and odd RF beams are

$$\phi_{m,\mathrm{Even}} = \arcsin\left(\frac{cm_{\mathrm{Even}}\tau_{1,\mathrm{Even}}}{d}\right) m_{\mathrm{Even}} = 0,1,\ldots,7 \quad (4a)$$

$$\phi_{m,\mathrm{Odd}} = \arcsin\left(\frac{cm_{\mathrm{Odd}}\tau_{1,\mathrm{Odd}}}{d}\right) m_{\mathrm{Odd}} = 0,1,\ldots,7 \quad (4b)$$

where d is the separation between antenna array T/R elements m_{Even} and m_{Odd} are the switch configurations for the even and odd beams, respectively. The minimum time delay associated with delay line 1 is directly related to the resolution of the beamformer. The minimum resolvable angle for both beams can be calculated by setting $m = 1$ in (4). So, in order to improve the angular resolution of the system, the minimum grating separation must be decreased thus leading to a shorter minimum time delay.

The presented two-beam two-channel beamformer is a proof of concept demonstration. Actual beamformers must be able to control antenna arrays with several elements and multiple beams. The PDM can be extended to control a linear antenna array with K T/R elements and M simultaneous RF beams. In the operation of an antenna array of K elements, the beamformer produces K linearly increasing time delays $\tau_i = (i-1)\Delta\tau$ with $\Delta\tau = d/c\sin\phi_0$ and $i = 1,\ldots,K$ to point the beam at an azimuth angle of ϕ_0, where d is the antenna T/R element separation and c speed of light. For multibeam operation with M independently driven beams, the beamforming network must be able to produce M independently time gradients $\Delta\tau_j = d/c\sin\phi_{0j}$ to point the beam j in the direction ϕ_{0j} with $j = 1,\ldots,M$[16]. The schematic of such multibeam N-bit PDM is shown in Fig. 2(b). The PDM consists of N delay lines in a binary configuration capable of process M RF beams in 2^N angular directions. Each delay line consists of M blocks with K Bragg reflectors each. Each block of FBG is used to provide the time delays that control one RF beam in a linear antenna array. The spacing between the gratings within a block is constant and it doubles from one delay line to the next. In each block, the center wavelengths of the Bragg reflectors match the International Telecommunications Union (ITU) channels, which are M channels apart. For example, the center wavelengths of the K reflectors in a block are designed to match the ITU channels X, $X+M$, $X+2M,\ldots,X+KM-1$ and $X+KM$. To be able to control each RF beam separately, M-port optical interleavers are used to demultiplex the optical channels. An M-port optical interleaver splits an incoming stream of dense WDM channels in M outputs being the channel spacing at the output M times the original channel spacing. The number of output ports of the interleaver limits the number of controllable RF beams. Commercially available optical interleavers with an interchannel spacing ratio of $50/400$ allow the PDM to steer up to eight RF beams. The switch units consist of M 1×2 optical switches and two $1 \times M$ fiber couplers, which are used to combine the outputs.

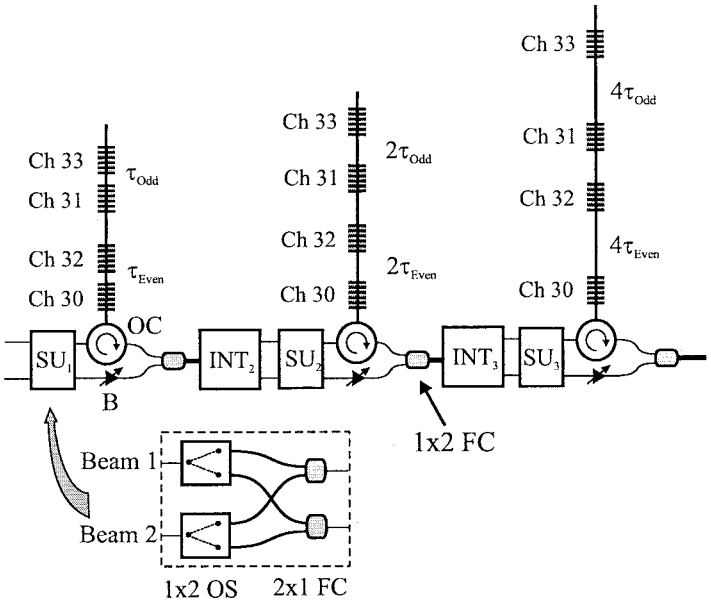

(a)

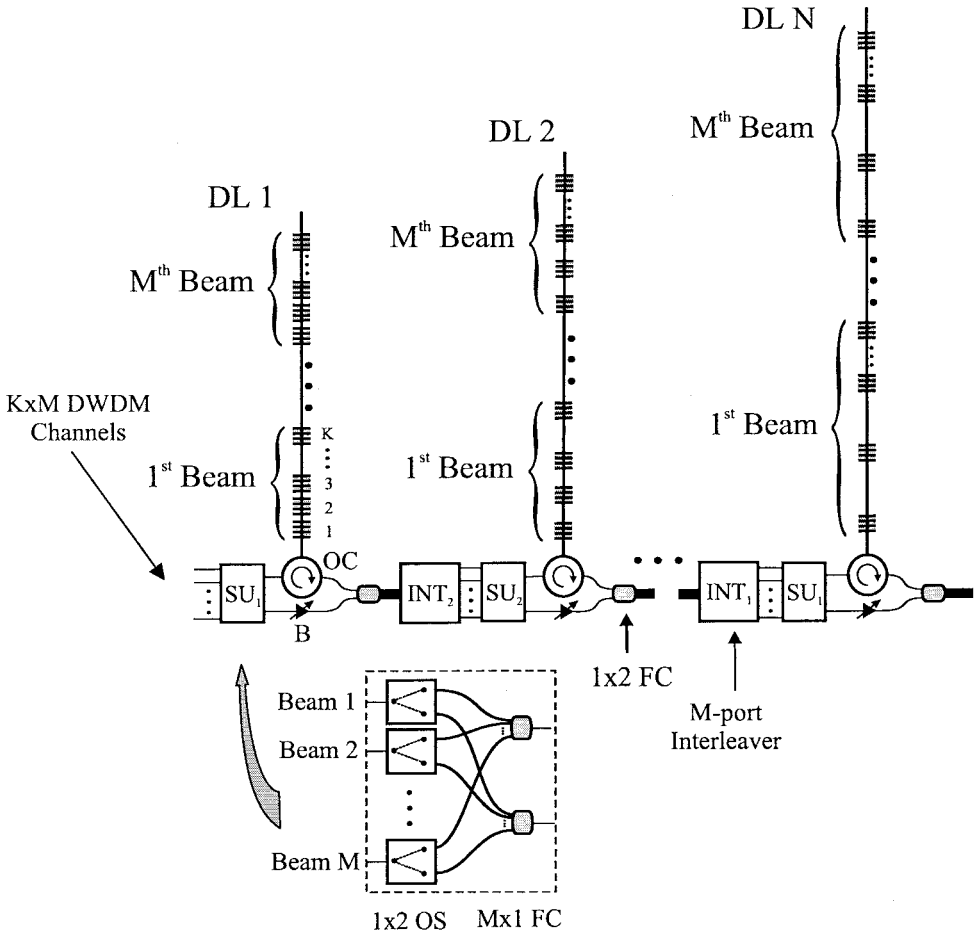

(b)

Fig. 2. (a) Two-beam two-channel 3-bit PDM in binary configuration. (b) K-channel M-beam N-bit version of the PDM. SU: Optical switch unit, OC: optical circulator, FC: fiber coupler.

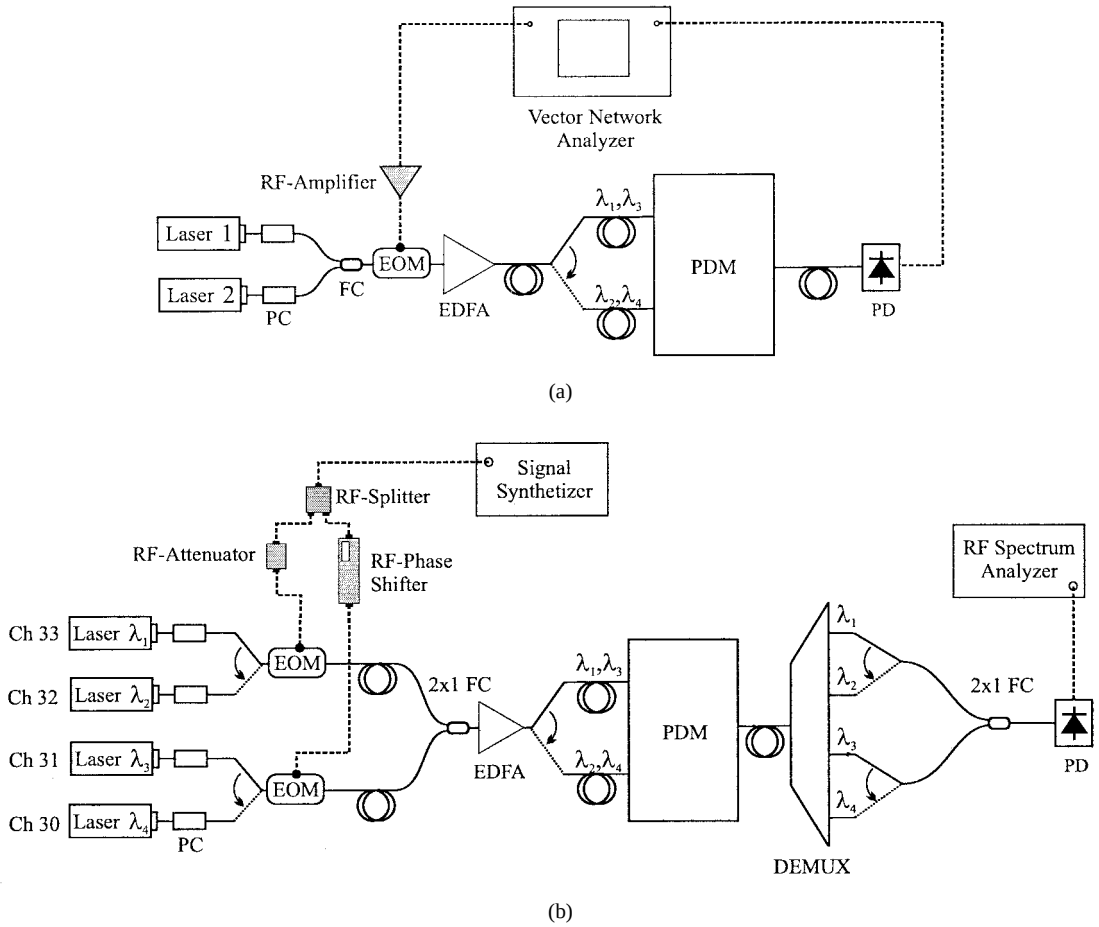

Fig. 3. (a) Optical setup for time-delay characterization. Diode lasers #1 and #2 match channels 30 and 32 (31 and 33) for even (odd) time-delay measurements. (b) Experimental setup for beam-pattern measurements simulating an incoming signal from a moving target. Since even and odd beams are characterized separately, the system is switched following the arrows between both measurements.

The ideal loss in a star $1 \times M$ fused fiber coupler is $10\log(M)$ decibels.

III. System Characterization

Each delay line consists of four FBG. The center wavelengths of the four gratings match the ITU frequency channels 30 ($\lambda_4 = 1553.33$ nm), 31 ($\lambda_3 = 1552.52$ nm), 32 ($\lambda_2 = 1551.72$ nm), and 33 ($\lambda_1 = 1550.92$ nm) with a maximum deviation of $\pm$ 0.1 nm. All the gratings have reflectivity from 97.75% to 99.84% and full-width at half-maximum (FWHM) between 0.4 and 0.6 nm. The minimum separation between the FBG associated with the even channels in line 1 is $\Delta L_{1,\mathrm{Even}} = 14 \pm 2$ mm. Separation for successive lines are 28 and 58 mm. For FBG of odd optical channels the minimum separation is 15 ± 2 mm, being 30 ± 2 mm and 60 ± 2 mm separation between odd FBG in lines 2 and 3, respectively. Using (3), the minimum time delay is calculated to be 137.11 ps for the even channels and 146.90 ps for the odd channels. Time delays associated with the remaining switch configurations are

$$\tau_{m,\mathrm{Even}} = m_{\mathrm{Even}} \cdot 137.11 \text{ ps}, \quad m_{\mathrm{Even}} = 0, 1, \ldots, 7 \tag{5a}$$

$$\tau_{m,\mathrm{Odd}} = m_{\mathrm{Odd}} \cdot 146.90 \text{ ps}, \quad m_{\mathrm{Odd}} = 0, 1, \ldots, 7. \tag{5b}$$

Optical circulators are used to route the signal between the delay lines and optical switches. A data acquisition unit that is interfaced with a computer controls these programmable optical switches. Based on the electronic control and switching time, the reconfiguration time for the PDM is 5 ms.

Time delays introduced by the PDM depend on the separation between FBG. Any variations of these separations cause a shift of the optical delays leading to a reduction in the performance of the beamformer. The system shown in Fig. 3(a) is used for measuring the actual time delays introduced by the PDM for each channel pair. Optical carriers, matching the wavelengths of ITU channels 30 though 33, are provided by semiconductor lasers. In-fiber polarization controllers set the proper polarization state at the input of the 10-GHz EOM. A particular pair of channels is modulated simultaneously with an RF signal. A vector network analyzer is used as a source to drive the RF signal to the EOM and to detect the RF signal from a 20-GHz photodiode. The phase and magnitude of the S_{12} parameter is compared for each individual channel providing the relation between phase difference and frequency given by

$$\Delta\varphi_m = \varphi_0 + 2\pi\tau_m\nu_{\mathrm{RF}} \tag{6}$$

where $\Delta\varphi_m$ is the phase difference between channels, φ_0 is an arbitrary constant phase, τ_m is the time delay, and ν_{RF} is the frequency of the signal. Experimental data is obtained by sweeping the frequency of the network analyzer between 0.2 and 1.6 GHz. Time delay is calculated from the slope of the linear fit to the unwrapped phase data using (6). The time delay is measured for

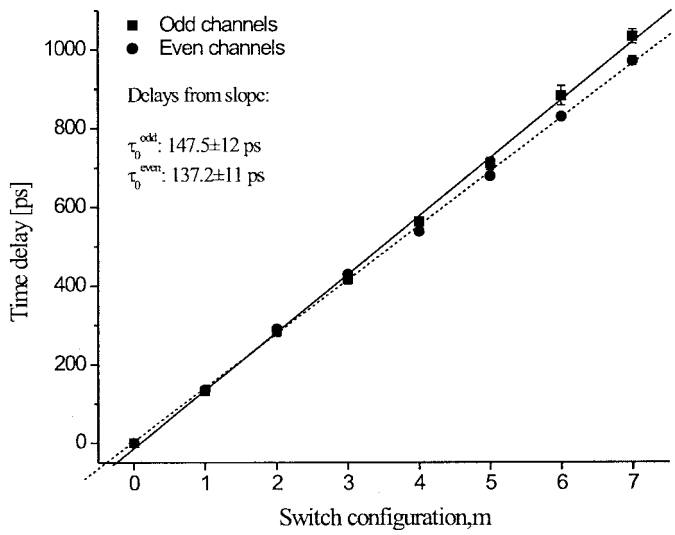

Fig. 4. Time-delay measurements associated to even and odd channels versus the switch configuration (parameter m) in the PDM. Lines show fit of experimental values to (5).

all possible switch configurations of PDM for both even and odd pairs of optical channels. The demultiplexer introduces a fixed additional amount of time delay between channels. This happens since WDM channels are dropped one at a time in a sequential way. Therefore, the time delay associated with the switch configuration $m = 0$ is not zero. Measurements of time delays due to the demultiplexer results in 15.71-ns delay between channels 33 and 30, 10.44-ns delay between channels 33 and 31, and 5.27-ns delay between channels 33 and 32. To obtain the corrected time delays, which are introduced only by the PDM, the measured time delay associated with $m = 0$ is subtracted from the measured time delays for the other switching configurations. Fig. 4 shows the measured time delays for the even and odd optical channels together with the theoretical curves given by (5). Notice that the standard deviation of the time-delay measurement is very small indicating that the system is capable of producing stable time delays for both RF beams. The measured minimum time delay for the even channels is 135.87 ps, which is a deviation of $-$ 0.90% from the assumed theoretical value. The measured minimum time delay for the odd channels is 132.24 ps, which is a deviation of $-$ 9.9% from the assumed theoretical value. In general, the deviations between the measured and theoretical time delays for all switch configurations of the PDM are less than 10.0% for the odd channels and less than 6.0% for the even channels. These deviations can be attributed to grating spacing errors. The linear behavior of the measured time delays for the even and odd channels shows that the time delay is proportional to the switching position m according to (5). The angular resolution, which is calculated from (4) by using the minimum measured time delay, is 7.1° for the odd beam and 6.9° for the even beam, where the corresponding theoretical values are 7.2° and 7.7°, respectively

If the beamformer steers the main lobe across a far-field observer located at broadside, the measured RF-power levels of the transmitted beams P_{Even} and P_{Odd} at the observer are given by (1). If isotropic radiating elements are assumed, (1) shows that the transmitted power depends on the time delays introduced by the PDM between the optical carriers through phase differences $\Delta\varphi_{\mathrm{Even}}$ and $\Delta\varphi_{\mathrm{Odd}}$, and the power of the optical carriers at the output of the system through constants K_{I}, K_{II}, K_{III}, K_{IV}. Since a uniform excitation of the array elements is assumed, the optical powers have to be independent of the switching configuration m of the PDM. A similar argument can be given for the transmit mode. However, in practice, optical losses through the PDM for each switch configuration are different. In order to achieve optical output powers that are independent of the switch configuration, channel balancers (optical attenuators) are added to the PDM. If a delay line is bypassed, the optical carrier neither passes through the circulator nor it is reflected by the FBG. Therefore, the insertion loss is quite different depending on whether the delay line is or is not in the path of the optical carrier. In addition, variations in the optical output power can also arise from different reflectivity of the FBG as well as wavelength-dependent insertion loss in the multiplexer. To provide equal loss levels, a channel balancer (optical attenuator) is placed in the bypass line, and the attenuation is set to compensate for the insertion loss of the circulator and the reflection loss of the FBG.

The measured optical insertion loss of the PDM is 35.4 dB that is close to the value 36.3 dB calculated using the specification data sheets of the components. Additional components, such as multiplexers and modulators with an approximate insertion loss of 3.7 and 6 dB, respectively, push the total insertion loss of the system to around 55 dB. To reduce the optical loss, an erbium-doped fiber amplifier (EDFA) with 26-dB gain is added in the system (see Fig. 1).

One of the main characteristics of TTD-controlled antenna systems is their large instantaneous bandwidth. The squint-free operation is experimentally verified by characterizing the array factor of the antenna for RF signals of different frequencies. The array factor is equivalent to the beam pattern when isotropic antenna T/R elements are considered. In this characterization, the PDM is fixed to one switching position and the output power of the system is measured while a simulated target moves past the antenna elements. The experimental setup is shown in Fig. 3(b). The performance of the PDM is tested for the two RF beams, one at a time. Crosstalk results of WDM channels in the system lead us to conclude that the two beam patterns can be measured separately with no significant difference in the performance of the beamformer. An RF-signal generator simulates an incoming RF beam from a target. The output of the signal generator is split and sent to two 10-GHz EOMs. An RF attenuator is used to compensate for any difference in the modulation performance of the two EOMs. To simulate the phase difference between antenna elements due to the moving target an RF phase shifter is introduced before one of the modulators. For each selected RF center frequency, the output signal from the photodiode is measured, using an RF spectrum analyzer, for 30 discrete phase-shifter settings. The phase shift sequence range from 0°/GHz to 900°/GHz. Fig. 5(a) shows the measured even and odd beam patterns along with fitted curves for three RF signals at 0.5, 1.0, and 1.5 GHz when the PDM is set to $m = 0$. At this particular switch position, the optical carriers do not pass through any of the delay lines of the PDM. For this reason, a

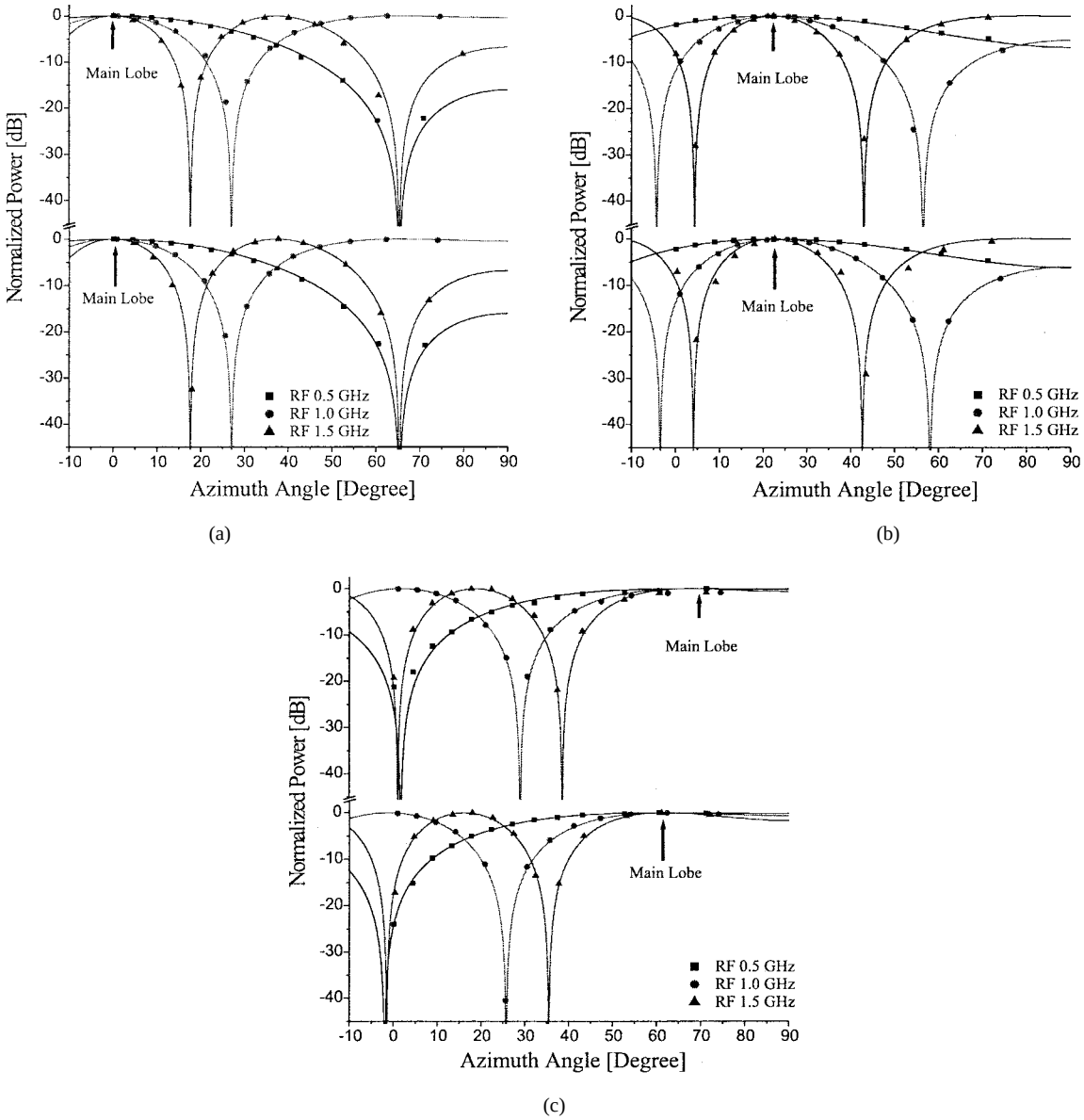

Fig. 5. Measured beam patterns for odd (top) and even (top) channels for RF center frequencies of 0.5, 1.0, and 1.5 GHz. The switch configuration of the PDM is $m = 0, 3$, and 7 for (a), (b), and (c), respectively. According to the value m, the main lobe is observed at 0°, 21.9°, and 60.7° for the even channels, and 0°, 23.6°, and 69.1° for the odd channels.

maximum in the output power is detected when the simulated target is at the broadside position. The angular direction or azimuth ϕ of the target is related to the phase difference $\Delta\varphi$ introduced by the phase shifter by

$$\phi = \arcsin\left(\frac{c\Delta\varphi}{2\pi\nu_{\mathrm{RF}}d}\right). \tag{7}$$

The antenna element spacing d is assumed as $0.5\lambda_{\mathrm{RF}}$ at 460 MHz, which, according to (4), allows the beamformer to process signals with azimuth angles up to 70° and 61° for odd and even beams, respectively. Fig. 5(a)–(c) shows beam patterns obtained for switching configurations $m = 1$, 3, and 7 of the PDM. In these cases, maximum output power is detected when the phase shift introduced by the phase shifter is compensated exactly by the phase shift produced by the PDM. These figures also show that the angular position of the main lobe, which is indicated by an arrow, for a given switch configuration coincide for the three RF beams. Beam patterns are measured and analyzed for the even and odd beams for all possible switch configurations. To demonstrate the large usable frequency range of the beamformer, beam patterns are analyzed for RF signals at 0.50, 0.75, 1.00, 1.25, and 1.50 GHz. To determine the position of the main lobe, the measured data points are fitted to (1) with a nonlinear curve-fit routine. The theoretical shift of the main lobe can be calculated using (4) and theoretical values of the minimum time delays in the PDM. Fig. 6 summarizes the angular main-lobe locations for incoming RF beams at several frequencies, which are processed by the even and odd channels for all possible switching configurations. Straight lines indicate the expected main lobe angular positions for each switch configuration. Error bars are calculated by measuring the beam pattern

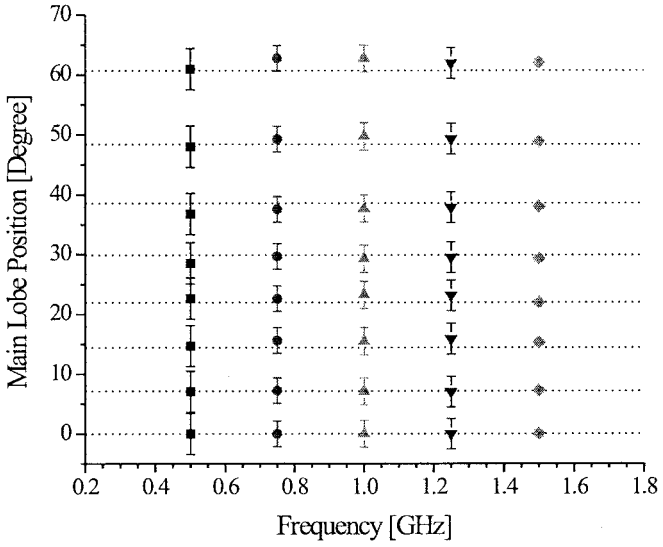

(a)

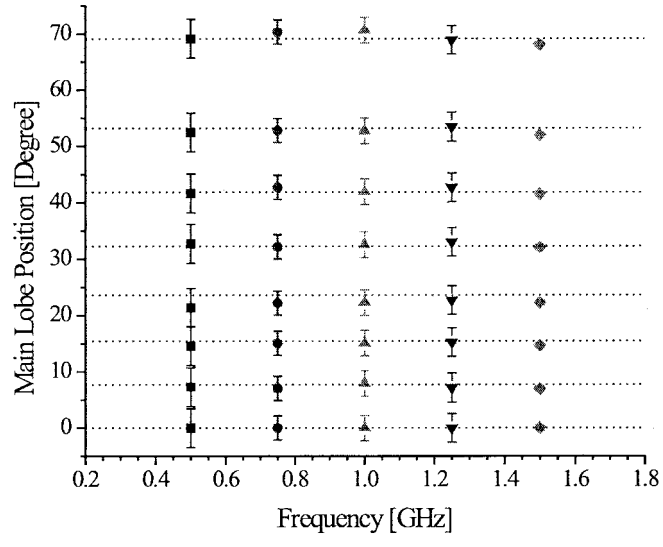

(b)

Fig. 6. Main-lobe locations versus RF center frequency for all possible PDM settings. (a) Even beam. (b) Odd beam. Solid lines (from bottom to top) indicate the theoretical main-lobe locations for switching positions $m = 0$ to 7. Squint-free performance is verified from 0.5 to 1.5 GHz.

and determining the location of the main lobe for each measurement. Maximum standard deviation of $\pm 3.4^\circ$ is calculated for the 0.5-GHz case. The measured main-lobe positions in Fig. 6 are independent of the frequency of the RF signal and show a good agreement with the predicted values. The deviation of the location of the main lobe from the theoretical values is less than $\pm 2.1^\circ$ for the even beam and less than $\pm 2.2^\circ$ for the odd beam.

IV. Transmit Mode Operation

Transmit mode measurements are performed using the configuration shown in Fig. 1(a). Even and odd carriers are modulated by EOM with RF signals provided by two signal generators. The detection scheme in Fig. 1(a) is slightly modified just for measurement purposes. The four carriers coupled at the output of the PDM are detected by a single photodetector. As the RF signals related to the even and odd channels have different frequencies, the RF power out of the photodetector for each beam is detected using an RF spectrum analyzer.

As it can be noted, RF signals in both even, respectively, odd carriers are in phase at the input of the PDM. The RF phase shift introduced by the PDM is transformed in power variations according to (1). These power variations represent the power of a signal received by an observer at 0° azimuth angular position for different switch configurations of the PDM. Consequently, beam patterns are characterized for an observer at the broadside position when the main lobe of the transmit beam is steered at three different angles.

Output RF powers for both beams are measured simultaneously for all the switching configurations. The steering angle, which corresponds to a given delay configuration, can be calculated from (4). Simultaneous transmit beam patterns for the odd RF beam at 1.5 GHz and the even RF beam at 0.6 GHz, together with the theoretical curves (even beam: solid line, odd beam: dotted line), are presented in Fig. 7(a). To illustrate the performance of the beamformer for two close RF center frequencies, Fig. 7(b) shows the beam pattern results for the even RF beam at 1.3 GHz and the odd RF beam at 1.4 GHz. To illustrate that both beams are simultaneously controlled by the beamformer, three selected spectral power profiles of the two detected RF center frequencies are shown below the beam patterns. To demonstrate that the two beams can be independently steered, the odd beam is steered from switching position $m_{\mathrm{Odd}} = 7$ trough 0 (which correspond to azimuth angles from 69° to 0°), while the even beam is steered from switching position $m_{\mathrm{Even}} = 0$ to 7 (corresponding to azimuth angles of 0° to 61°). Even though measured data points show good agreement with the theoretical curves, deviation of the measured power levels from theoretical beam patterns can be noted. These deviations are larger for the odd RF beam than for the even RF beam; in particular, the error bars are higher for the odd case.

V. Receive-Mode Operation

For this set of measurements, it is assumed that two RF beams are received simultaneously with the beamformer from targets at fixed azimuth positions ϕ_{Odd} and ϕ_{Even}. In order to detect the angular position of each target, the power of the output RF signal from the beamformer is measured as the PDM sweeps through all the possible delay configurations for both beams.

The experimental setup used for receive measurements is a modified version of the system shown in Fig. 1(b). As before, two RF synthesizers simulate the incoming RF beams from two targets. The signal related to the incoming even RF beam is split in two signals. One of the signals, after passing through an RF attenuator to compensate for both EOMs, modulates the optical channel 32. The remaining signal, that modulates the optical channel 30, passes through an RF-phase shifter, which introduces a phase delay simulating the angular position of the even target. Note that according to (7), the incoming angle for an RF

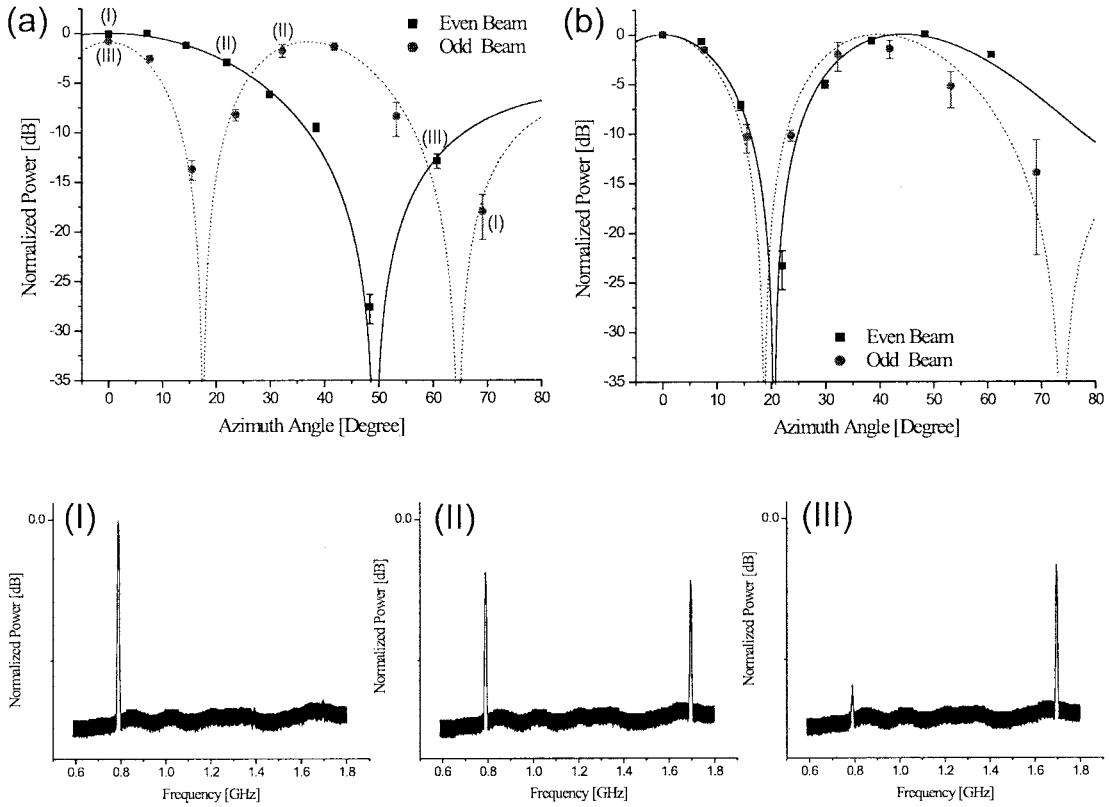

Fig. 7. Transmit simultaneous beam patterns for: (a) even beam at 0.6 GHz and odd beam at 1.5 GHz; (b) even beam at 1.3 GHz and odd beam at 1.4 GHz. Below the beam patterns are selected spectral power profiles for the case (a). Each profile is related to a particular switch configuration of the PDM and its number is related to values in the beam pattern. The profile (I) is measured for switch configuration $m_{\mathrm{Even}} = 0$, $m_{\mathrm{Odd}} = 7$, profile (II) for $m_{\mathrm{Even}} = 3$, $m_{\mathrm{Odd}} = 4$, and profile (III) for $m_{\mathrm{Even}} = 7$, $m_{\mathrm{Odd}} = 0$.

beam can be calculated from the phase difference $\Delta\varphi$ between antenna elements. Due to the limited availability of EOM, odd optical channels are coupled and modulated with the RF signal from the second synthesizer using a single 3-GHz EOM. Since the RF signals modulated on optical channels 31 and 33 are in phase, a broadside-incoming beam is always simulated in the odd case, i.e., $\phi_{\mathrm{Odd}} = 0$. The RF signals out of the PDM are demodulated and detected by a single photodetector and an RF spectrum analyzer.

Measurements are performed for two simultaneous incoming RF beams with frequencies of 0.6 and 1.5 GHz. The switching configurations are swept from $m = 0$ to 7 synchronously for both beams in order to detect the position of both targets. Three cases are considered for three different positions of the even target by maintaining the odd target stationary. Fig. 8(a) shows the measured receive beam pattern for the odd RF beam at a frequency of 0.6 GHz. Data points representing the normalized RF power output are plotted against the azimuth angles related to the phase delay introduced by the PDM at each switch configuration. A maximum in the curve is noticed at an azimuth angle of 0° as it is expected from the fact that the odd target is supposed at broadside. Fig. 8(b) shows the results for the even RF beam. The sequence of simulated angular positions are $\phi_{\mathrm{Even}} = 0°$, 20.7°, and 56.7° which correspond to values of the phase shifter of $\Delta\varphi = 0°$, 210°, and 495°. In all cases, the solid line is the theoretical curve from (1) fitted to the experimental points. The angles obtained by the fit are 0°, 20.7°, and 57.4°, which show a good agreement with theory. It can be noted from Fig. 8 that data points related to the odd RF beam have larger error bars than the ones related to the even RF beam. For the case of odd RF beam, only the last four points exhibit large power variations. For these switch configurations, optical carriers are routed through the third delay line and the performance of the odd channels is affected. On the other hand, the performance of even channels is independent of the switching position of the PDM. Our analysis reveals that these high deviations are attributed to power variations due to optical interference of odd channels. This is caused by multiple reflections between Bragg reflectors of channels 31 and 33 with the FBG of channel 32. Note that the error bars are plotted in decibels, therefore, for small power values the error bars seem much larger than for high power values, even if the standard deviation for both measured powers is the same.

VI. Discussion and Conclusion

We have proposed a multibeam optical beamformer capable of driving a phased-array antenna in receive and transmit modes.

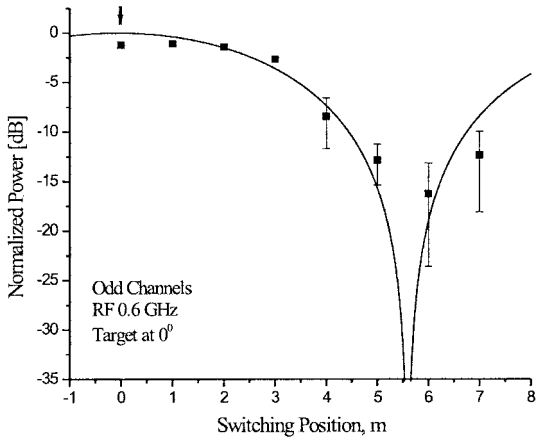

(a)

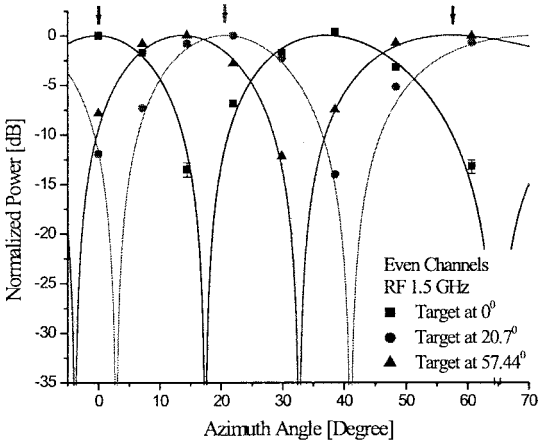

(b)

Fig. 8. Measured simultaneous beam patterns in receive mode. (a) Odd incoming RF beam pattern at 0.6 GHz. In this case, the target is detected at broadside. (b) Even RF beam patterns at 1.5 GHz for three different simulated positions of the target. The even target is detected at 0°, 20.7°, and 57.44°.

The PDM can be programmed to sweep the antenna aperture following an independent angular sequence for each RF beam. A simpler two-beam two-channel version of the beamformer has been demonstrated. The system is based on an array of three delay lines, which gives the antenna an angular resolution of 3 bits. That is, two beams can be pointed independently in eight different angular directions. Each delay line is composed of four FBG matching the channels 30 to 33 of the ITU grid. The possible angular range of the antenna is 0° to 61° when the RF beam is processed with the even optical channels and 0° to 70° when the RF beam is processed with the odd optical channels.

Measurements are performed for the receive and transmit modes and for RF center frequency between 0.5 and 1.5 GHz. The measurements are limited to 1.5 GHz to obtain a reasonable amount of data points per beam lobe. The transmit mode is characterized for a broadside target across which the two RF beams are steered. In the receive mode, the beamformer is characterized simulating and detecting two RF beams from targets. Results for both transmit and receive measurements show good agreement with the theoretical model. Due to crosstalk between FBG of delay line 3, odd optical channels show larger deviations from the theoretical curves than the even channels. This problem can be solved selecting FBG with smaller bandwidth. Squint-free operation of the beamformer is demonstrated for RF center frequency between 0.5 and 1.5 GHz for both the even and odd RF beams.

Notice that no additional optical components such as circulators, switches, or attenuators will be necessary to scale up this proposed PDM for phased-array antennas with a large number of T/R elements. This upgrade only requires an increase in the number of FBG in each delay line. However, the total insertion loss (IL) of the PDM will increase significantly as the number of RF beams and delay lines increase following the expression $IL[\text{dB}] \propto N \cdot (10 \log 1/M + IL_{\text{Res}})$, where IL_{Res} is the total loss of one delay line. This total loss is the sum of contribution from the circulator, 3-dB coupler, the optical switch, and the interleaver. The total number of required optical channels is proportional to the number of RF beams and antenna elements. Consequently, the number of available WDM channels limits the number of RF beams that can be processed by antennas with large number of T/R elements. However, stable multiwavelength broad-band laser sources combined with reduction in the interchannel spacing of WDM technology to 25 GHz or less can partially overcome these limitations.

REFERENCES

[1] N. Riza, Ed., *Selected Papers on: Photonics Control Systems for Phased Array Antennas*. Bellingham, WA: SPIE, 1997, vol. MS 136, SPIE Milestone Series.

[2] A. P. Goutzoulis, D. K. Davies, and J. M. Zomp, "Prototype binary fiber optic delay line," *Opt. Eng.*, vol. 28, pp. 1193–1202, 1989.

[3] N. A. Riza and N. Madamopoulos, "Phased array antenna maximum compression reversible photonic beamformer," *Appl. Opt.*, vol. 36, pp. 983–996, 1997.

[4] S. Palit, M. Jaeger, S. Granieri, A. Siahmakoun, B. Black, and J. Chestnut, "5-bit programmable binary and ternary architectures for an optical transmit/receive beamformer," *IEICE Trans. Fundamentals*, to be published.

[5] R. Soref, "Fiber grating prism for true time delay beamsteering," *Fiber Integr. Opt.*, vol. 15, pp. 325–333, 1996.

[6] H. Zmuda, A. Soref, P. Payson, S. Johns, and E. Toughlian, "Photonic beamformer for phased array antennas using a fiber grating prism," *IEEE Photon. Technol. Lett.*, vol. 9, pp. 241–243, Feb. 1997.

[7] R. Esman, M. Frankel, J. L. Dexter, L. Goldberg, M. G. Parent, D. Stilwell, and D. G. Cooper, "Fiber-optic prism true time delay antenna feed," *IEEE Photon. Technol. Lett.*, vol. 5, pp. 1347–1349, Nov. 1993.

[8] D. Tong and M. Wu, "Transmit/receive module of multiwavelength optically controlled phased-array antennas," *IEEE Photon. Technol. Lett.*, vol. 10, pp. 1018–1020, 1998.

[9] S. Palit, S. Granieri, A. Siahmakoun, B. Black, and C. Pagel, "Performance characteristics of 5-bit optical receive beamformer," in *Proc. SPIE: Applications of Photonics Technology V*, vol. 4833, 2002, pp. 348–353.

[10] P. J. Matthews, M. Y. Frankel, and R. D. Esman, "A wide-band fiber-optic true-time-steered array receiver capable of multiple independent simultaneous beams," *IEEE Photon. Technol. Lett.*, vol. 10, pp. 722–724, May 1998.

[11] G. A. Koepf, "Optical processor for phased-array antenna beam formation," *Proc. SPIE*, vol. 477, pp. 75–81, 1984.

[12] Y. Ji, K. Inagaki, R. Miura, and Y. Karasawa, "Optical processor for multibeam microwave receive array antennas," *Electron. Lett.*, vol. 32, pp. 822–824, 1996.

[13] Y. Ji, K. Inagaki, O. Shibata, and T. Karasawa, "Receive mode of optical signal processing multibeam array antennas," *IEEE Microwave Guided Wave Lett.*, vol. 8, pp. 251–253, July 1998.
[14] O. Shibata, K. Inagaki, Y. Karasawa, and Y. Mizuguchi, "Spatial optical beamforming network for receiving-mode multibeam array antenna: Proposal and experiment," *IEEE Trans. Microwave Theory Tech.*, vol. 50, pp. 1425–1430, May 2002.
[15] N. Riza, "An acousto-optic phased-array antenna beamformer for multiple simultaneous beam generation," *IEEE Photon. Technol. Lett.*, vol. 4, pp. 807–809, July 1992.
[16] H. Zmuda and E. N. Toughlian, *Photonic Aspects of Modern Radar*. Boston, MA: Artech House, 1994.

S. Granieri received the B.S. and Ph.D. degrees in physics from the University of La Plata, La Plata, Argentina, in 1993 and 1998, respectively. His doctoral research focused on the study and optical generation of the fractional Fourier transform and applications to signal processing.

From 1994 to 1998, he worked at Optical Research Center (CIOp), La Plata, Argentina, where he has engaged in research on optical information processing. From 1998 to 2000, he was assigned to the Optical Communication Laboratory (LAMECO) at the same institution, where he pursued research on erbium-doped fiber amplifiers. Since 2000, he has been with the Rose-Hulman Institute of Technology, Terre Haute, IN, where he has been principally involved with research on optical control of phased-array antennas for radar applications and optical analog/digital conversion.

M. Jaeger received the B.S. degree in electrical engineering from the University of Stuttgart, Stuttgart, Germany, in 2000, and the M.S. degree in applied optics from the Rose-Hulman Institute of Technology, Terre Haute, IN, in 2002.

His research interests are in the area of radio frequency photonics, optical analog/digital conversion, and optical communication systems.

A. Siahmakoun (M'00) received the B.S. degree from Jondi Shahpoor University, Iran, in 1978, the M.S. degree from Texas A&I (now Texas A&M), Kingsville, in 1981, and the Ph.D. degree from the University of Arkansas, Fayetteville, in 1987, all of which are in physics.

He joined the Department of Physics and Applied Optics of the Rose-Hulman Institute of Technology, Terre Haute, IN, in September 1987, where he is now a Professor of physics and optical engineering and the Director of the Center for Applied Optics Studies. He has been active in optics education and research and has recently developed a microfabrication and microelectromechanical systems (MEMS) laboratory for teaching undergraduate students. He is the Principal Investigator of Wideband Optical Beamformer and Optical Delta-Sigma Modulator that are supported by the Office of Naval Research (ONR) 2000–2005. His research interests are in the areas of optical MEMS, radio frequency photonics, optical analog-to-digital conversion, and optical information processing.